$$\frac{1}{L}\int_0^L m^2 \mathrm{d}x = \frac{1}{(1+\alpha^2)^{1/2}} = I_1 + I_2; \quad \frac{1}{L}\int_0^L n^2 \mathrm{d}x = 1 - \frac{1}{(1+\alpha^2)^{1/2}} = 1 - I_1 - I_2, \tag{9}$$

$$\frac{1}{L}\int_0^L n^4 \mathrm{d}x = 1 - \frac{2+3\alpha^2}{2(1+\alpha^2)^{3/2}} = 1 - I_1 - 2I_2, \tag{10}$$

$$\frac{1}{L}\int_0^L m^3 n \mathrm{d}x = \frac{1}{L}\int_0^L m n^3 \mathrm{d}x = \frac{1}{L}\int_0^L m^3 n \mathrm{d}x = \frac{1}{L}\int_0^L mn \mathrm{d}x = 0, \tag{11}$$

where

$$\alpha = 2\pi \frac{A}{L}. \tag{12}$$

Accordingly, the components in Eq. (5) can be explicitly expressed as:

$$\bar{C}_{1111} = I_1\left(C^*_{1111} - C^*_{2222}\right) + 2I_2\left(C^*_{1122} - C^*_{2222} + 2C^*_{1212}\right) + C^*_{2222}, \tag{13}$$
$$\bar{C}_{1122} = I_2\left(C^*_{1111} - 2C^*_{1122} + C^*_{2222} - 4C^*_{1212}\right) + C^*_{1122}, \tag{14}$$
$$\bar{C}_{1133} = I_1\left(C^*_{1122} - C^*_{2233}\right) + I_2\left(C^*_{1122} - C^*_{2233}\right) + C^*_{2233}, \tag{15}$$
$$\bar{C}_{2211} = I_2\left(C^*_{1111} - 2C^*_{1122} + C^*_{2222} - 4C^*_{1212}\right) + C^*_{1122}, \tag{16}$$
$$\bar{C}_{2222} = I_1\left(C^*_{2222} - C^*_{1111}\right) + I_2\left(2C^*_{1122} + 4C^*_{1212} - 2C^*_{1111}\right) + C^*_{1111}, \tag{17}$$
$$\bar{C}_{2233} = I_1\left(C^*_{2233} - C^*_{1122}\right) + I_2\left(C^*_{2233} - C^*_{1122}\right) + C^*_{1122}, \tag{18}$$
$$\bar{C}_{3311} = (I_1 + I_2)\left(C^*_{1122} - C^*_{2233}\right) + C^*_{2233}, \tag{19}$$
$$\bar{C}_{3322} = (I_1 + I_2)\left(C^*_{2233} - C^*_{1122}\right) + C^*_{1122}, \tag{20}$$
$$\bar{C}_{3333} = C^*_{3333}, \tag{21}$$
$$\bar{C}_{1212} = I_2\left(C^*_{1111} - 2C^*_{1122} + C^*_{2222} - 4C^*_{1212}\right) + C^*_{1212}, \tag{22}$$
$$\bar{C}_{2323} = (I_1 + I_2)\left(C^*_{2323} - C^*_{1212}\right) + C^*_{1212}, \tag{23}$$
$$\bar{C}_{1313} = (I_1 + I_2)\left(C^*_{1212} - C^*_{2323}\right) + C^*_{2323}. \tag{24}$$

The effective longitudinal Young's modulus in the 1-direction, $\bar{E}_1$, is given as:

$$\bar{E}_1 = \frac{1}{\bar{D}_{1111}}, \quad \text{where} \quad \bar{\mathbf{D}} = \bar{\mathbf{C}}^{-1}. \tag{25}$$

Based on Eq. (25) and a simple volume summation, the reinforcing capability of wavy CNT is evaluated by the following equation ([1,26,34]):

$$E_{\text{wavy}} = \lim_{\phi \to 0} \frac{\bar{E}_1 - (1-\phi)E^0}{\phi}. \tag{26}$$

Figure 2 shows the variations of E_{wavy} associated with the waviness factor, $w = A/L$. As clearly displayed, the fiber waviness significantly lowers the effectiveness of CNT. The present analysis tends to estimate higher modulus compared to the FEM analysis [26] in particular for $E^1/E^0 = 1,000$ as exhibited by Fig. 2a. Further, Fig. 2b illustrates the extent of relative degradation, E_{wavy}/E^1, and the present analysis is relatively insensitive to the value of E^1/E^0. The obtained result in Fig. 2a is similar to the result reported by Anumandla and Gibson [34].

To reproduce Eq. (5) with the Mori–Tanaka method, we substitute $\mathbf{C}^* = \bar{\mathbf{C}}$ and $\mathbf{S} = \bar{\mathbf{S}}$ in Eq. (1) as follows:

$$\bar{\mathbf{C}} = \mathbf{C}^0 \bullet \left\{\mathbf{I} + \phi\left[(\mathbf{C}^1 - \mathbf{C}^0)^{-1} \bullet \mathbf{C}^0 + (1-\phi)\bar{\mathbf{S}}\right]^{-1}\right\}. \tag{27}$$

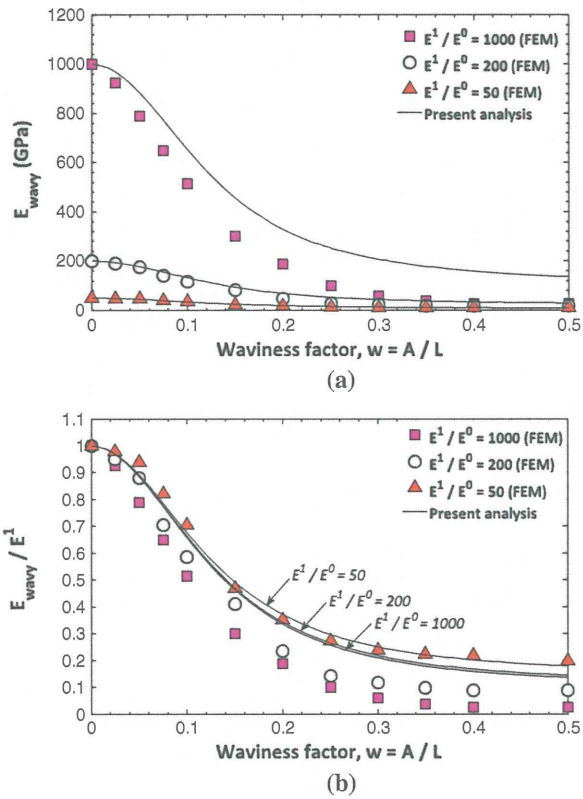

Fig. 2 Variations in reinforcing effect with fiber waviness [26]. **a** Effect of waviness on E_{wavy}. **b** Effect of waviness on E_{wavy}/E^1. $\nu^1 = 0.3$, $E^0 = 1.0$ GPa, $\nu^0 = 0.3$

Therefore, based on Eqs. (5) and (27), we can express $\bar{\mathbf{S}}$ as

$$\bar{\mathbf{S}} = \lim_{\phi \to 0} \frac{1}{1-\phi} \left[\phi \left((\mathbf{C}^0)^{-1} \bullet \bar{\mathbf{C}} - \mathbf{I} \right)^{-1} - (\mathbf{C}^1 - \mathbf{C}^0)^{-1} \bullet \mathbf{C}^0 \right], \tag{28}$$

where $\bar{\mathbf{S}}$ is termed as an ad hoc Eshelby tensor that can account for the effect of fiber waviness. To exclude the effect of far-field interaction in the Mori–Tanaka method, we take the limit in Eq. (28) (i.e., dilute concentration, cf. [24,25,30]). It is noted that, strictly speaking, the Eshelby tensor is constant only when the inclusion shape is ellipsoid [32]; thus, Eq. (28) is essentially an ad hoc solution for the wavy fiber. In what follows, the effects of waviness on the effective elastic responses are examined by employing the ad hoc Eshelby tensor while Fisher et al. [1,26] used the reduced effective CNT moduli with straight fiber via finite element method to reflect the effects of waviness.

2.2 Effective elastic stiffness of multi-phase composites

Since Eq. (28) is based on the planar sinusoidal fiber, we consider the random orientation of CNT about the 1-axis in Fig. 1 by the following equation:

$$S^*_{ijkl} = \frac{1}{2\pi} \int_0^{2\pi} Q_{ip} Q_{jq} Q_{kr} Q_{ls} \bar{S}_{pqrs} \mathrm{d}\psi, \quad \text{where} \quad Q_{ij} = \begin{bmatrix} 1 & 0 & 0 \\ 0 & \cos\psi & -\sin\psi \\ 0 & \sin\psi & \cos\psi \end{bmatrix}. \tag{29}$$

Equation (29) is essential to reproduce the isotropy of randomly oriented fiber-reinforced composites. According to Eq. (29), the following relations are obtained:

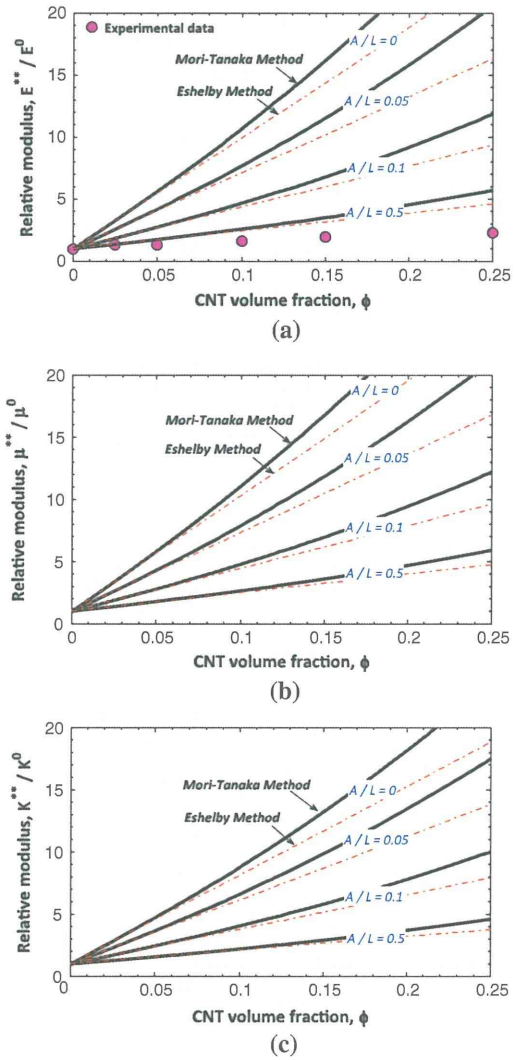

Fig. 3 Effects of CNT volume fraction on the effective elastic moduli of CNT–polystyrene composites [35] (cf. [1,34]). **a** Variations of effective Young's modulus, E^{**}. **b** Variations of effective shear modulus, μ^{**}. **c** Variations of effective bulk modulus, K^{**}. $E^1 = 1.0$ TPa, $\nu^1 = 0.3$, $E^0 = 1.9$ GPa, $\nu^0 = 0.3$

$$S^*_{1111} = \bar{S}_{1111}, \tag{30}$$

$$S^*_{1122} = S^*_{1133} = \frac{1}{2}\left(\bar{S}_{1122} + \bar{S}_{1133}\right), \tag{31}$$

$$S^*_{2211} = S^*_{3311} = \frac{1}{2}\left(\bar{S}_{2211} + \bar{S}_{3311}\right), \tag{32}$$

$$S^*_{2222} = S^*_{3333} = \frac{1}{8}\left(3\bar{S}_{2222} + \bar{S}_{2233} + \bar{S}_{3322} + 3\bar{S}_{3333} + 4\bar{S}_{2323}\right), \tag{33}$$

$$S^*_{2233} = S^*_{3322} = \frac{1}{8}\left(\bar{S}_{2222} + 3\bar{S}_{2233} + 3\bar{S}_{3322} + \bar{S}_{3333} - 4\bar{S}_{2323}\right), \tag{34}$$

$$S^*_{1212} = S^*_{1313} = \frac{1}{2}\left(\bar{S}_{1212} + \bar{S}_{1313}\right), \tag{35}$$

$$S^*_{2323} = \frac{1}{8}\left(\bar{S}_{2222} - \bar{S}_{2233} - \bar{S}_{3322} + \bar{S}_{3333} + 4\bar{S}_{2323}\right). \tag{36}$$

It is noted that only when $A = 0$ (i.e., straight fiber), $\mathbf{S} = \bar{\mathbf{S}} = \mathbf{S}^*$ holds.

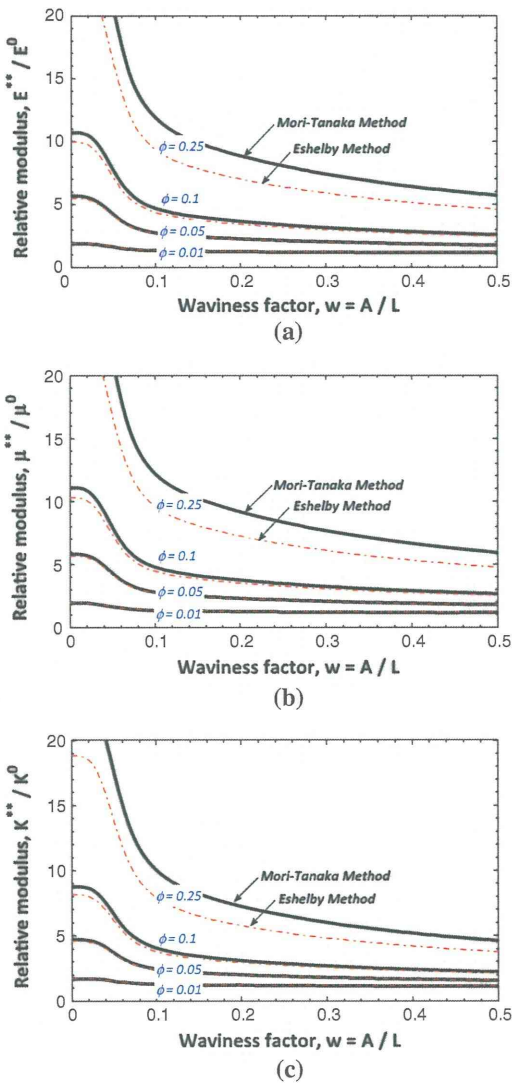

Fig. 4 Effects of waviness factor on the effective elastic moduli of CNT–polystyrene composites. **a** Variations of effective Young's modulus, E^{**}. **b** Variations of effective shear modulus, μ^{**}. **c** Variations of effective bulk modulus, K^{**}. $E^1 = 1.0$ TPa, $\nu^1 = 0.3$, $E^0 = 1.9$ GPa, $\nu^0 = 0.3$

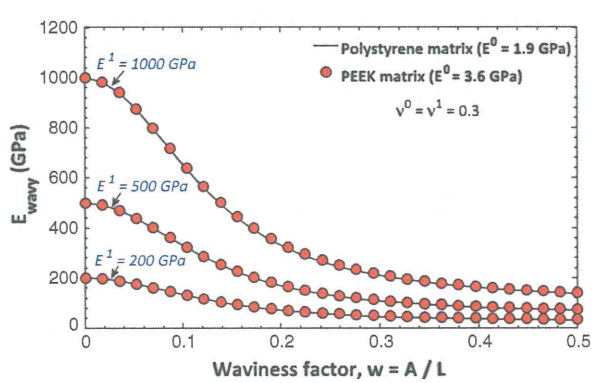

Fig. 5 Variations in reinforcing effect with fiber waviness for different matrix materials

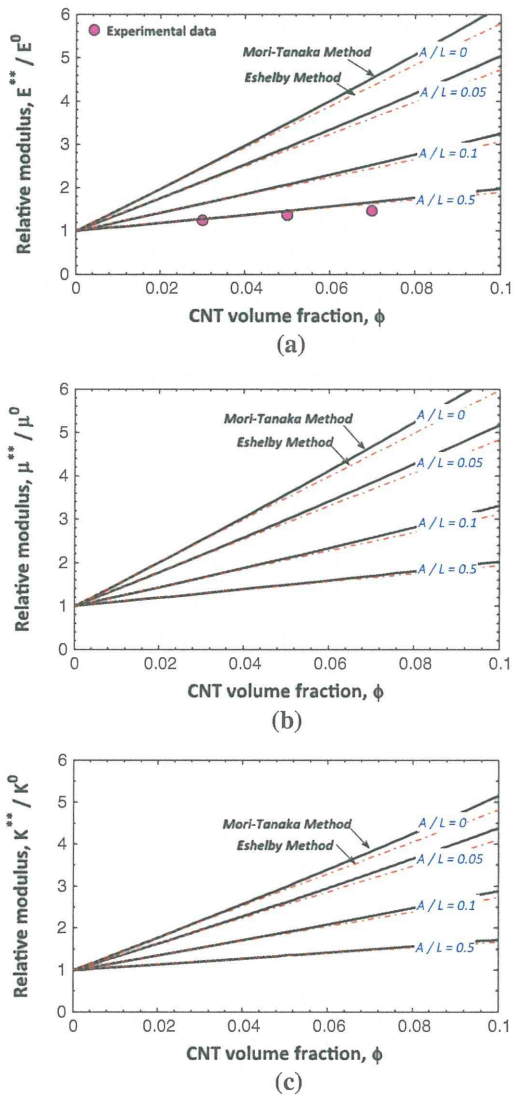

Fig. 6 Effects of CNT volume fraction on the effective elastic moduli of CNT–PEEK composites. **a** Variations of effective Young's modulus, E^{**}. **b** Variations of effective shear modulus, μ^{**}. **c** Variations of effective bulk modulus, K^{**}. $E^1 = 1.0$ TPa, $\nu^1 = 0.3$, $E^0 = 1.9$ GPa, $\nu^0 = 0.3$

Based on the Mori–Tanaka method, the effective stiffness for the multiphase composites is rendered as [30]:

$$\mathbf{C}^{**} = \left[(1-\phi)\mathbf{C}^0 + \sum_{r=1}^{N} \phi^r \mathbf{C}^r \bullet \mathbf{T}^r\right] \bullet \left[(1-\phi)\mathbf{I} + \sum_{n=1}^{N} \phi^n \mathbf{T}^n\right]^{-1}, \tag{37}$$

where

$$\mathbf{T}^r = \mathbf{I} - \left[\mathbf{I} + (\mathbf{C}^r - \mathbf{C}^0)^{-1} \bullet \mathbf{C}^0 \bullet (\mathbf{S}^*)^{-1}\right]^{-1}. \tag{38}$$

To simulate the randomly oriented wavy CNT fiber-reinforced composites, we modify Eq. (37) as:

$$\mathbf{C}^{**} = \left[(1-\phi)\mathbf{C}^0 + \phi\langle \mathbf{C}^1 \bullet \mathbf{T}^1\rangle\right] \bullet \left[(1-\phi)\mathbf{I} + \phi\langle \mathbf{T}^1\rangle\right]^{-1}, \tag{39}$$

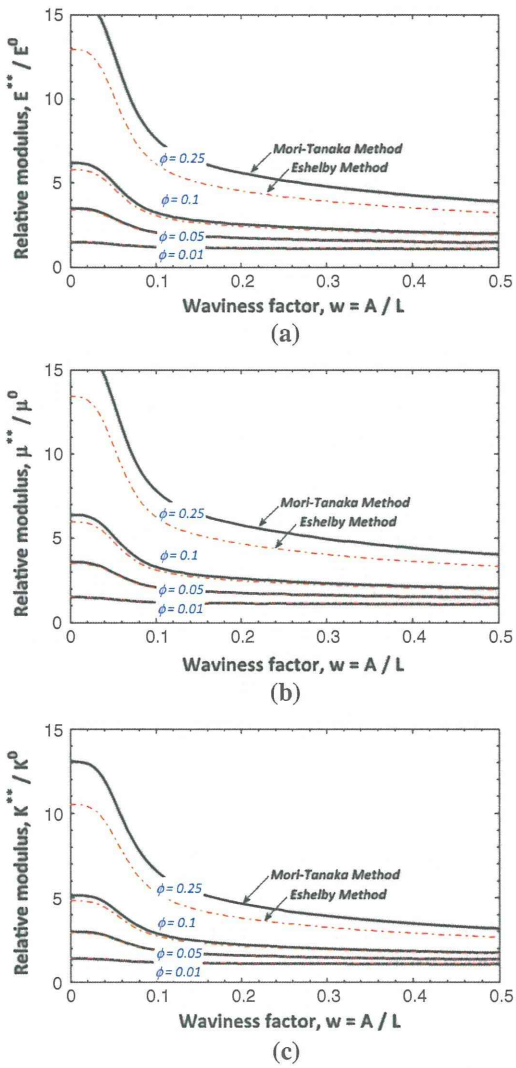

Fig. 7 Effects of waviness factor on the effective elastic moduli of CNT–PEEK composites. **a** Variations of effective Young's modulus, E^{**}. **b** Variations of effective shear modulus, μ^{**}. **c** Variations of effective bulk modulus, K^{**}. $E^1 = 1.0$ TPa, $\nu^1 = 0.3$, $E^0 = 3.6$ GPa, $\nu^0 = 0.3$

where

$$\mathbf{T}^1 = \mathbf{I} - \left[\mathbf{I} + (\mathbf{C}^1 - \mathbf{C}^0)^{-1} \bullet \mathbf{C}^0 \bullet (\mathbf{S}^*)^{-1}\right]^{-1}. \tag{40}$$

In Eq. (39), $\langle \bullet \rangle$ signifies the orientational averaging for a fourth-order tensor and takes the form

$$\langle M \rangle_{ijkl} = \frac{1}{\pi} \int_0^{\pi} \left(\int_0^{\pi/2} Q_{ip} Q_{jq} Q_{kr} Q_{ls} M_{pqrs} \cos\varphi \mathrm{d}\varphi \right) \mathrm{d}\theta, \tag{41}$$

where

$$Q_{ij} = \begin{bmatrix} \cos\theta\cos\varphi & \sin\theta & \cos\theta\sin\varphi \\ -\sin\theta\cos\varphi & \cos\theta & -\sin\theta\sin\varphi \\ -\sin\varphi & 0 & \cos\varphi \end{bmatrix}. \tag{42}$$

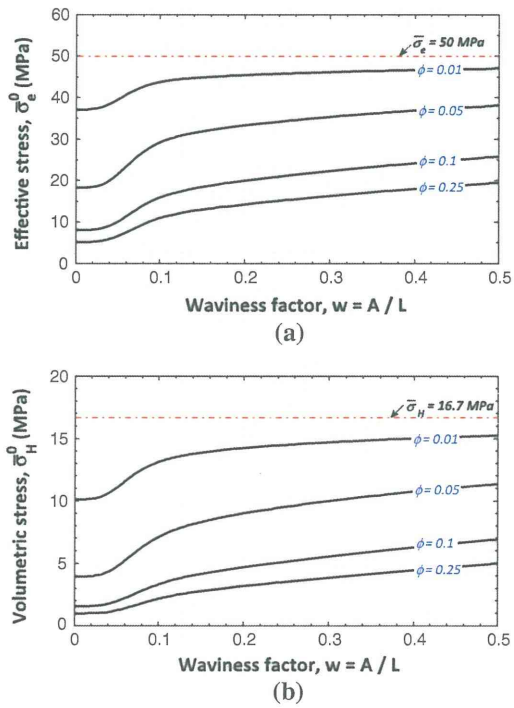

Fig. 8 Effects of waviness factor on the stress norms of CNT–PEEK composites under the uniaxial loading condition $\bar{\sigma}_{11} = 50$ MPa. **a** Variations of effective stress in the matrix. **b** Variations of volumetric stress in the matrix. $E^1 = 1.0$ TPa, $\nu^1 = 0.3$, $E^0 = 3.6$ GPa, $\nu^0 = 0.3$

After a straightforward calculation, the following relations can be obtained:

$$\langle M\rangle_{ijkl} = c_1\delta_{ij}\delta_{kl} + c_2(\delta_{ik}\delta_{jl} + \delta_{il}\delta_{jk}),$$

where

$$c_1 = \frac{1}{30}(2M_{1111} + 3M_{1133} + 8M_{3311} + 10M_{3322} + 2M_{3333} - 8M_{1313}), \tag{43}$$

$$c_2 = \frac{1}{60}(4M_{1111} + M_{1133} - 4M_{3311} - 10M_{3322} + 14M_{3333} + 24M_{1313}). \tag{44}$$

On the other hand, the Eshelby method (i.e., dilute concentration method, cf. [30]) renders the effective stiffness as

$$\mathbf{C}^{**} = \mathbf{C}^0 + \phi\langle(\mathbf{C}^1 - \mathbf{C}^0) \bullet \left[\mathbf{I} + \mathbf{S}^* \bullet \left((\mathbf{C}^0)^{-1} \bullet \mathbf{C}^1 - \mathbf{I}\right)\right]^{-1}\rangle. \tag{45}$$

By using Eqs. (39) or (45), the effective elastic moduli of isotropic composites are calculated as:

$$E^{**} = \frac{C_{1212}^{**}(3C_{1122}^{**} + 2C_{1212}^{**})}{C_{1122}^{**} + C_{1212}^{**}}; \quad \mu^{**} = C_{1212}^{**}; \quad K^{**} = C_{1122}^{**} + \frac{2C_{1212}^{**}}{3}, \tag{46}$$

where E^{**}, μ^{**}, and K^{**} are the effective Young's modulus, shear modulus, and bulk modulus, respectively. In this study, the isotropic CNT is assumed though the anisotropic CNT [9] can be equally handled with the proposed micromechanical framework.

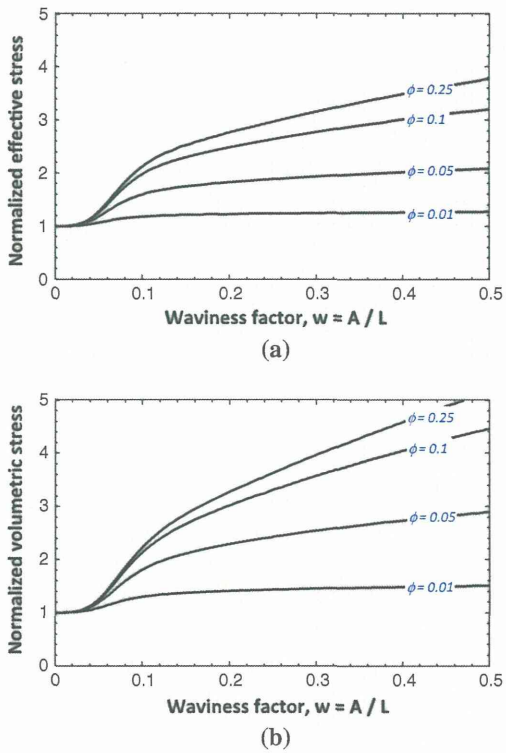

Fig. 9 Effects of waviness factor on the normalized stress norms of CNT–PEEK composites under the uniaxial loading condition $\bar{\sigma}_{11} = 50$ MPa. **a** Variations of normalized effective stress of the matrix. **b** Variations of normalized volumetric stress of the matrix. $E^1 = 1.0$ TPa, $\nu^1 = 0.3$, $E^0 = 3.6$ GPa, $\nu^0 = 0.3$

2.3 Overall stress norms of matrix

Similar to Eq. (39), by taking advantage of orientational averaging, the global stress concentration tensor for the matrix material, $\mathbf{B}^0$, can be written as [30]:

$$\bar{\boldsymbol{\sigma}}^0 = \mathbf{B}^0 : \bar{\boldsymbol{\sigma}} = \left[(1-\phi)\mathbf{I} + \phi\langle \mathbf{C}^1 \bullet \mathbf{T}^1 \bullet (\mathbf{C}^0)^{-1}\rangle\right]^{-1} : \bar{\boldsymbol{\sigma}}. \tag{47}$$

In contrast to metals, polymeric solids generally exhibit pressure-dependent yield behavior. This is evidenced by a significant increase in yield stress with hydrostatic pressure and a lower yield stress in simple tension compared to that in simple compression. Therefore, both the effective stress and the volumetric stress influence the elastoplastic behavior of CNT-reinforced polymer composites. Based on Eq. (47), the volumetric stress, $\bar{\sigma}_H^0$, and the effective stress, $\bar{\sigma}_e^0$, for the matrix are computed as:

$$\bar{\sigma}_H^0 = \frac{1}{3}\bar{\sigma}_{kk}^0; \quad \bar{\sigma}_e^0 = \sqrt{\frac{3}{2}\bar{\sigma}_{ij}^{0\prime}\bar{\sigma}_{ij}^{0\prime}}, \quad \text{where} \quad \bar{\sigma}_{ij}^{0\prime} = \left(I_{ijkl} - \frac{1}{3}\delta_{ij}\delta_{kl}\right)\bar{\sigma}_{kl}^0. \tag{48}$$

3 Results and discussions

Figure 3 shows the effect of CNT volume fraction on the effective elastic moduli of CNT–polystyrene composites. Because of the specific high elastic modulus of CNT, the increased amount of far-field interaction (cf. [30]) can be expected even for dilute concentration of CNT. However, by comparing the predictions by the Eshelby method and the Mori–Tanaka method, they are close to each other only for the dilute concentration of CNT (e.g., $\phi = 0.05$), which is usually observed for the conventional composite materials. Concerning the effect of fiber waviness, as the waviness factor, $w = A/L$, increases, the predictions by the Eshelby method and the Mori–Tanaka method become indistinguishable in conjunction with the reduced amount of the far-field

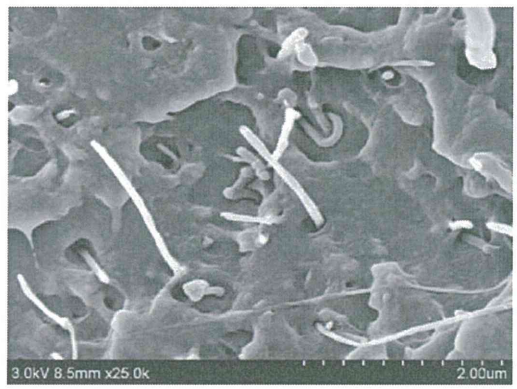

(a)

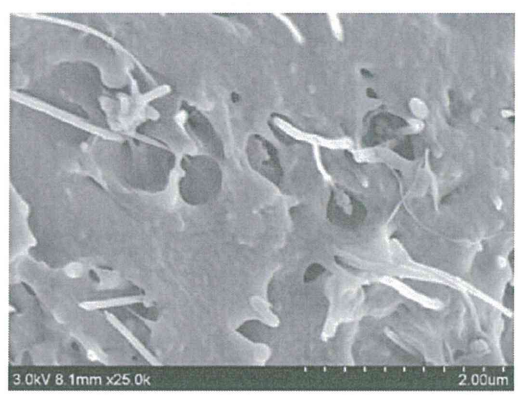

(b)

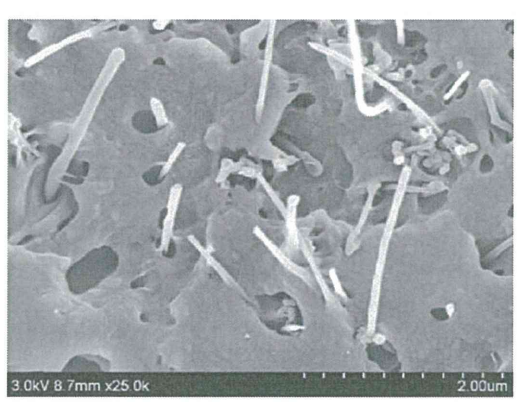

(c)

Fig. 10 SEM images of the cross sections of CNT–PEEK composites. **a** CNT volume fraction $\phi = 0.03$. **b** CNT volume fraction $\phi = 0.05$. **c** CNT volume fraction $\phi = 0.07$

interaction. As clearly exhibited, compared to the prediction with straight fiber (i.e., $A/L = 0$), the experimental data ([35], cf. [1,34]) are discouraging. Figure 4 illustrates the influence of waviness. As shown, the waviness has a pronounced effect, and small waviness (e.g., $A/L = 0.1$) substantially affects the mechanical behavior of composites, in particular for high CNT volume fraction. Somewhat similar observation was reported by Fisher et al. [26].

Polyether ether ketone (PEEK) is an organic polymer thermoplastic used in engineering applications. PEEK is recognized as an advanced biomaterial used in medical implants, and it is also widely used in the aerospace,

automotive, teletonic, and chemical process industries. In this research, by aiming for bioengineering applications, the mechanical responses of CNT–PEEK composites are investigated. The influence of elastic matrix modulus on the load-transfer capability of wavy fiber is examined in Fig. 5. Irrespective of matrix modulus, identical degradation of E_{wavy} (cf. Eq. (26)) is observed. Figures 6 and 7 show the effect of CNT volume fraction and CNT waviness on the effective elastic moduli of CNT–PEEK composites. Similar to Fig. 3a, the experimental data in Fig. 6a are disappointing compared to the prediction with straight fiber (i.e., $A/L = 0$). By comparing Figs. 3, 4, 5, 6, and 7, a notable distinction due to the difference of elastic moduli of matrix material (polystyrene vs. PEEK) cannot be observed.

Figure 8 displays the effects of the waviness factor on the stress norms of CNT–PEEK composites under the uniaxial loading condition. The increased amount of CNT effectively reduces the stress norms, which is beneficial to prevent the matrix yielding. Associated with Fig. 8, Fig. 9 illustrates the variations of normalized stress norms. As exhibited, the matrix with higher CNT volume fraction is more sensitive to the CNT waviness, primarily due to the increased amount of CNT.

Finally, Fig. 10 renders the SEM images of CNT–PEEK composites. As is clearly seen, numerous porosities can be observed around the CNTs. Accordingly, it is expected that the imperfect interfaces significantly influence the mechanical responses of composites. Moreover, CNT agglomeration [9] can be observed for $\phi = 0.07$ (cf. Fig. 10c). Nevertheless, the incorporation of CNTs can still enhance the mechanical properties of composites, as demonstrated by Fig. 6a. This would be due to the specific high elastic modulus of CNT. Given the moderate waviness observed in Fig. 10, the incorporation of small CNT volume fraction seems promising to enhance the mechanical properties of composites if the interface property can be improved (cf. $A/L = 0.1$ in Fig. 6). The present research is undertaken not only to investigate the mechanical responses of composites, but also to examine the biocompatibility of composites. Hence, in view of the biocompatibility, the porosities shown in Fig. 10 may serve as the conglutination sites for human tissues though the toxicity of CNT for bioengineering applications should be carefully examined.

4 Concluding remarks

In this study, the effects of CNT waviness on the effective elastic responses of CNT–polymer composites are investigated. By taking advantage of the ad hoc Eshelby tensor, the micromechanical field equations are systematically presented. Based on a series of parametric studies with the micromechanics-based closed form solution, the significance of CNT waviness is discussed. According to the present predictions and the experimental evidences, the importance of load transfer at the imperfect interfaces and the promise of CNT–polymer composites are acknowledged.

Acknowledgments The first and second authors are supported by Japanese Health Labour Sciences Research (Grant No. KB240013). The third author is in part sponsored by the Faculty Research Grant of the Academic Senate of UCLA (Fund Number 4-592565-19914) and in part by Bellagio Engineering.

References

1. Fisher, F.T., Bradshaw, R.D., Brinson, L.C.: Fiber waviness in nanotube-reinforced polymer composites—I: Modulus predictions using effective nanotube properties. Compos. Sci. Technol. **63**, 1689–1703 (2003)
2. Andrews, R., Weisenberger, M.C.: Carbon nanotube polymer composites. Curr. Opin. Solid State Mater. Sci. **8**, 31–37 (2004)
3. Harris, P.J.F.: Carbon nanotube composites. Int. Mater. Rev. **49**(1), 31–43 (2004)
4. Andrews, R., Jacques, D., Minot, M., Rantell, T.: Fabrication of carbon multiwall nanotube/polymer composites by shear mixing. Macromol. Mater. Eng. **287**, 395–403 (2002)
5. Cadek, M., Coleman, J.N., Barron, V., Hedicke, K., Blau, W.J.: Morphological and mechanical properties of carbon-nanotube-reinforced semicrystalline and amorphous polymer composites. Appl. Phys. Lett. **81**(27), 5123–5125 (2002)
6. Lau, K.-T., Hui, D.: Effectiveness of using carbon nanotubes as nano-reinforcements for advanced composite structures. Carbon **40**, 1597–1617 (2002)
7. Wong, M., Paramsothy, M., Xu, X.J., Ren, Y., Li, S., Liao, K.: Physical interactions at carbon nanotube-polymer interface. Polymer **44**, 7757–7764 (2003)
8. Bai, J.: Evidence of the reinforcement role of chemical vapour deposition multi-walled carbon nanotube in a polymer matrix. Carbon **41**, 1309–1328 (2003)
9. Barai, P., Weng, G.J.: A theory of plasticity for carbon nanotube reinforced composites. Int. J. Plast. **27**, 539–559 (2011)
10. Allaoui, A., Bai, S., Bai, H.M., Bai, J.B.: Mechanical and electrical properties of a MWNT/epoxy composite. Compos. Sci. Technol. **62**, 1993–1998 (2002)
11. Kulkarni, M., Carnahan, D., Kulkarni, K., Qian, D., Abot, J.L.: Elastic response of a carbon nanotube fiber reinforced polymeric composite: a numerical and experimental study. Compos. Part B **41**, 414–421 (2010)